



Snow Particle Fragmentation Enhances Snow Sublimation

Ning Huang^{1,3}, Jiacheng Bao^{1,3}, Hongxiang Yu², and Guang Li²

¹College of Civil Engineering and Mechanics, Lanzhou University, Lanzhou, China

²College of Atmospheric Sciences, Lanzhou University, Lanzhou, China

³The Ministry of Educational Department, Key Laboratory of Mechanics on Disaster and Environment in Western China, Lanzhou, China

Correspondence: Hongxiang Yu (yuhx2023@lzu.edu.cn); Guang Li (lg@lzu.edu.cn)

Abstract. Fragmentation of snow particles, where dendritic snowflakes transform into spherical shapes upon impact with surface and other particles during drifting and blowing snow events, plays a critical role in shaping snow dynamics. This phenomenon is important because it influences the size distribution and concentration of snow particles, affecting mass flux and sublimation rates. Currently, prevailing drifting and blowing snow models ignore the snow particles fragmentation, leading to heightened uncertainties in predicting flow structures and sublimation rates. Here, we aim to quantitatively investigate the impact of snow particle fragmentation on sublimation. We establish a drifting and blowing snow model considering the snow particle fragmentation process and investigated the effects of fragmentation on drifting and blowing snow. The results show that fragmentation enhances the sublimation of blowing snow and changes the airborne particle size distribution. The sublimation rate of saltating snow particles increases 11 % on average, and that of suspension snow particles increases 76 % on average, when the friction wind speed is between 0.3 m/s to 0.5 m/s. These findings have important implications for improving the physical dynamic model of drifting and blowing snow, which may contribute to predictions in snow hydrology and climate models.

1 Introduction

Snow plays an important role in Earth's climate system because of its wide coverage and seasonal variation, leading to variable surface conditions. Sublimation is a significant way for snow surface to transfer the heat, mass, and energy with the atmosphere. Snow sublimation includes static snow cover sublimation and dynamical snow particles sublimation in air transportation. The latter process contains drifting snow sublimation (DSS) or blowing snow sublimation (BSS). Water vapor transport in DSS has a significant influence on the local hydrological cycle and distribution, especially in the polar region and high alpine regions. For example, in Antarctica coastline area, water loss caused by drifting and blowing snow reaches 18.3 % of the whole drifting and blowing snow amount each year (Pomeroy and Jones, 1996). In the Tibet Plateau, due to its special environmental condition, the sublimation amount is severely high, and it takes about 50 % of the amount of snow cover every year (Ueno et al., 2007).

Sublimation of snow particles is closely related to particle size, shape, and specific area of particle (Domine et al., 2009). Sublimation changes with particle size, meanwhile, the sublimation rate is affected by the particle size. When



25 snow particles move in the air, their size will not only be diminished due to sublimation but also could be breakage due to collision with the surface and other particles. The phenomenon wherein particles collide with a surface during saltation, resulting in the separation and deformation of the snowflakes into smaller-sized snow particles, is referred to as fragmentation. The fragmentation not only changes the size distribution of the snow granular system but also changes the snowpack's physical properties such as the surface albedo of snow cover (Domine et al., 2006).

30 There is only one model (Comola et al., 2017) considering the fragmentation of the snow particles during the drifting snow. This work using a statistical mechanics model calculated the fragmented number of particles from the perspective of energy and mass balance and simply analyzed the effects of fragmentation on the particle size distribution. However, in that work, the influence of fragmentation on the drifting snow flux and subsequent snow sublimation has not been investigated. It is therefore essential to incorporate the fragmentation process into a
35 physical numerical model to quantitatively assess its effect on snow particle sublimation, especially from the micro-scale perspective of individual particles experiencing dynamic size changes during their movement.

In the previous numerical models, snowflakes have typically been represented as rigid spheres with a constant diameter. However, given that snowflakes are easily deformed and fragile granular materials, their diameters continuously change during saltation in the air (Sato et al., 2008; Walter et al., 2024). Consequently, the impact of
40 the dynamically evolving size distribution of snow particles cannot be ignored in the numerical simulation. This is particularly crucial for accurately estimating sublimation rates and quantities, as a precise characterization of the dynamically changing size of particles is fundamentally important.

2 Model description

A comprehensive drifting and blowing snow model was well developed by Huang and Shi (2017). It described the
45 saltating snow particles near the surface in a Lagrangian way and the suspended snow particles above the surface in an Eulerian way. A threshold grain size was used to judge the saltating and suspended particles. The Thorpe and Mason model (Thorpe and Mason, 1966) was used to calculate the sublimation of drifting and blowing snow. The feedback of particle motion and particle sublimation to the wind field, air temperature, and air humidity were also considered. Particle fragmentation was now taken into consideration in the saltation splash process. Here, we
50 reintroduced them briefly.

2.1 Air flow

Considering the steady state of saltation, the horizontal wind field satisfies the following equations (Nemoto and Nishimura, 2004):

$$\frac{\partial}{\partial z}(\rho_f \kappa^2 z^2 \left| \frac{du}{dz} \right| \frac{du}{dz}) + f_p = 0 \quad (1)$$



55 where z is height over the surface, ρ_f is air density, κ is von Karman constant, u is wind speed, and f_p is the feedback force of the airborne snow particles.

The air temperature and humidity equations satisfying the horizontal uniformity condition follow (Bintanja, 2000b):

$$\frac{\partial \theta}{\partial t} = \frac{\partial}{\partial z} (K_\theta \frac{\partial \theta}{\partial z}) + S_\theta \quad (2)$$

60 where θ is air potential temperature, $K_\theta = \kappa u_* z + K_T$ is the heat turbulent coefficient, K_T is the molecular diffusion coefficients of heat, and S_θ is the sublimation heat feedback of the airborne snow particles.

$$\frac{\partial q_v}{\partial t} = \frac{\partial}{\partial z} (K_q \frac{\partial q_v}{\partial z}) + S_q \quad (3)$$

where q_v is water vapor mixing ratio, $K_q = \kappa u_* z + K_v$ is the water vapor turbulent coefficient, K_v is the molecular diffusion coefficient of water vapor, S_q is the sublimation humidity feedback of the airborne snow particles.

65 2.2 Snow saltation

The motion of saltating snow particles can be described as five sub-processes:

(1) Aerodynamic entrainment

The snow particles start to move when wind speed reaches a certain value (namely fluid threshold, usually presented by friction velocity) for a certain snow surface, which is called aerodynamic entrainment. The ratio of aerodynamic
70 entrainment is known as a linear function of the surface shear stress τ (Anderson and Haff, 1991):

$$N_a = A(\tau - \tau_t) \quad (4)$$

where N_a is the number of aerodynamic entrainment particles per unit area per second, $A[N^{-1}s^{-1}]$ is an empirical coefficient, and τ_t is threshold surface shear stress. The particle size distribution $f(d)$ follows the Gamma Distribution:

$$f(d) = \frac{d^{\alpha-1}}{\beta^\alpha \Gamma(\alpha)} e^{-d/\beta} \quad (5)$$

75 There are two ways to judge the motion pattern of snow particles. The most used way is to set up a threshold height to divide the saltation layer and suspension layer, which is easy to apply. However, the threshold value is empirical and has big differences among different literatures. The other way is determined by the particle size, which is based on the followability. The lifting velocity of aerodynamic entrainment particles is set as $\sqrt{2gd}$ (Dai and Huang, 2014), which is not sensitive to the steady state of saltation.

80 (2) Particle's trajectory



After the snow particles are lifted into the air, their trajectories can be described by Newton's second law:

$$m \frac{d\mathbf{r}}{dt} = \mathbf{f}_d - m\mathbf{g} \quad (6)$$

where m is the mass of the snow particle, $\mathbf{r}(x, z)$ is the location of the particle, \mathbf{f}_d is the drag force by fluid, \mathbf{g} is the gravitational acceleration.

85 (3) Splash function

In this model, we use the probability functions to describe the movement after particle impacting the surface (Sugiura and Maeno, 2000). The restitution coefficient in the vertical direction $S_v(e_v)$, the restitution coefficient in the horizontal direction $S_h(e_h)$ and the number of particles ejected from the surface n_e follows these functions:

$$S_v(e_v) = \frac{e_v^{a-1}}{b^a \Gamma(a)} e^{-\frac{e_v}{b}} \quad (7)$$

$$90 \quad S_h(e_h) = \frac{1}{\sqrt{2\pi}\sigma^2} e^{-\frac{(e_h-\mu)^2}{2\sigma^2}} \quad (8)$$

$$n_e = C_m^{n_e} p^{n_e} (1-p)^{m-n_e} \quad (9)$$

inwhich v_{ix} is the horizontal component velocity of the impact grain, v_{iy} is the vertical component velocity of the impact grain, v_{ex} is the horizontal component velocity of the jump grain, and v_{ey} is the vertical component velocity of the jump grain. $e_v = v_{ey}/v_{iy}$ is the vertical recovery coefficient, $e_h = v_{ex}/v_{ix}$ is the horizontal recovery coefficient, n_e

95 is the number of jumping snow grains. $S_v(e_v)$ is the probability distribution function of e_v , $S_h(e_h)$ is the probability distribution function of e_h , and $S_e(n_e)$ is the probability distribution function of n_e . $\Gamma(a)$ is the gamma function, $C_m^{n_e} = m!/[n_e!(m-n_e)!]$ is the combination number. the probability for particles break after impact (Comola et al., 2017) is calculated as

$$p(f) = 1 - \frac{1}{\sqrt{1 + \frac{\sigma^2}{w_s}}} \quad (10)$$

100 in which, σ^2 is the turbulence velocity variance and w_s is the settling velocity of snow particles. When a snow particle falls back to the ground (initial velocity $v_i > 0.5$ m/s), use Equation 10 to determine whether it is broken, and then calculate the number of snow particles N and λ is the ratio of particle size before and after fragmentation as (Comola et al., 2017) :

$$\begin{cases} N = 15v_i - 2.5, 0.5 < v_i < 1.5 \\ N = \frac{5}{7}(6v_i + 19), v_i > 1.5 \end{cases} \quad (11)$$



105

$$\begin{cases} \lambda = -0.4v_i + 0.7, 0.5 < v_i < 1.0 \\ \lambda = -0.1v_i + 0.4, 1.0 < v_i < 1.5 \\ \lambda = 0.25, v_i > 1.5 \end{cases} \quad (12)$$

The velocity of the newly produced snow particles after crushing is the same as the size of the snow particles that are broken, and the direction angle of the exit velocity is the same as that of the original snow particles.

(4) Sublimation

110 The drifting snow sublimation is calculated by the Thorpe and Mason model (Thorpe and Mason, 1966):

$$\frac{dm}{dt} = \frac{\pi d(RH - 1) - \frac{Q_r}{KNuT} \left(\frac{L_s}{R_v T} - 1 \right)}{\frac{L_s}{KNuT} \left(\frac{L_s}{R_v T} - 1 \right) + \frac{R_v T}{ShDe_s}} \quad (13)$$

where m is the particle mass, d is the particle diameter, T is the air temperature, RH is the air relative humidity, Q_r is the solar radiation which snow particles absorbed, K is the heat conductivity, R_v is the gas constant of water vapor (461.5 J/kg/K), D is the molecular diffusivity of water vapor, e_s is the saturated vapor pressure relative to the ice surface, Nu is the Nussel number and Sh is the Sherwoods number.

(5) Feedback to air

The airborne particles have a significant effect on airflow. To consider this effect, we used an equivalent body force:

$$\mathbf{f}_p = -\frac{1}{V} \sum_{i=1}^N \mathbf{f}_{di} \quad (14)$$

120 where f_p is the feedback body force of the airborne particles in a vertical grid, V is the volume of this vertical grid, N is the number of the airborne particles in this vertical grid, f_{di} is the drag force of the i_{th} particle in the grid.

The volume sublimation rate in each grid can be calculated as:

$$S = -\frac{1}{V} \sum_{i=1}^N \frac{dm_i}{dt} \quad (15)$$

where m_i is the mass of the i_{th} particle in the grid.

125 Then, the sublimation feedback to air temperature and humidity are:

$$S_\theta = -\frac{L_s S}{\rho_f C} \quad (16)$$

$$S_q = \frac{S}{\rho_f} \quad (17)$$

where $L_s = 2.84 \times 10^6$ J/kg is the latent heat of sublimation, S is the volume drifting and blowing snow sublimation rate, and $C = 1006$ J/kg K is the specific heat of air.

130

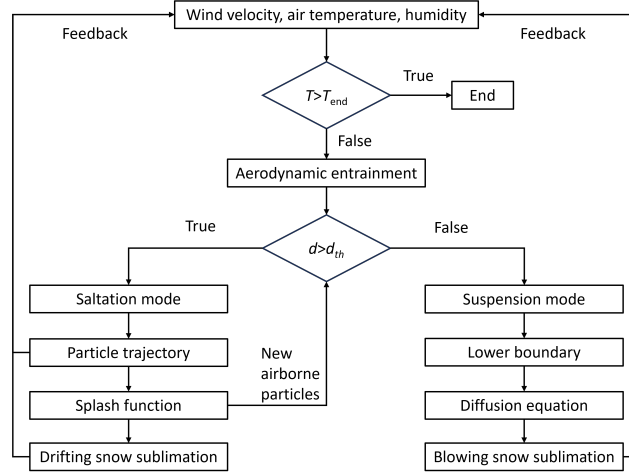


Figure 1. Flowchart of the new drifting and blowing snow model

2.3 Snow suspension

In the simulation, we define a threshold radius for judging suspension and saltation particles (Huang and Shi, 2017), the threshold radius is calculated by the Rouse number:

$$R_N = \frac{w_s}{\kappa u_*} \quad (18)$$

in which, u_* is the friction velocity and w_s is the particle deposit terminal velocity. Therefore, the conditions for determining the saltation and suspension snow particles (Scott, 1995) :

$$\begin{cases} R_N > 1, \text{saltation} \\ R_N \leq 1, \text{suspension} \end{cases}$$

135 The suspended snows follow the vertical diffusion equation (Déry and Yau, 2002):

$$\frac{\partial q_s}{\partial t} = \frac{\partial}{\partial z} \left(K_s \frac{\partial q_s}{\partial z} + w_s q_s \right) + S \quad (19)$$

where q_s is the suspended snow particle mixing ratio, $K_s = \delta \kappa u_* z$ is the diffusion coefficient of suspended particles, w_s is the terminal velocity. The δ follows (Csanady, 1963):

$$\delta = \frac{1}{\sqrt{1 + \frac{\beta^2 f^2}{w'^2}}} \quad (20)$$

140 where $\beta = 1$ is the proportionality constant, w' is the vertical turbulent fluid velocity, and we set $\overline{w'^2} = u_*^2$. A flowchart is shown as Fig.1 to present how this new splash function works.

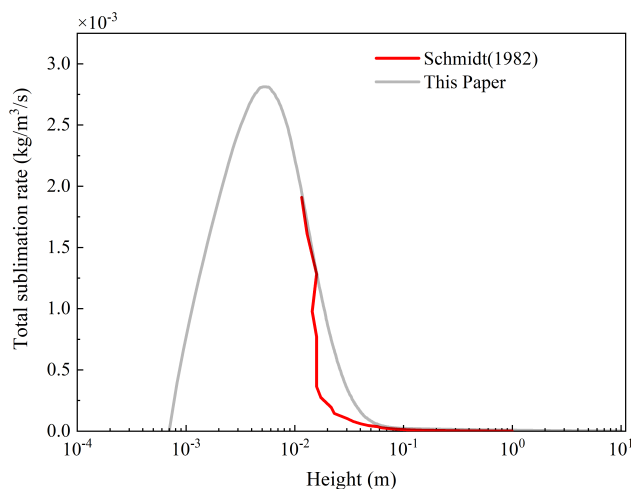


Figure 2. Comparison of total sublimation rate for this paper and field observation (Schmidt, 1982) ($u_* = 0.63$ m/s, $z_0 = 7 \times 10^{-4}$ m, $T = 267.45$ K)

2.4 Model verification

To verify the model, we compared sublimation rate and mass concentration.

Fig. 2 shows the comparison of the total sublimation rate between the numerical simulation and the field observa-
145 tion data. The red curve is the sublimation rate of the field observation, and the gray curve is the simulation result
of the sublimation rate under the same conditions. Comparing the two curves, we can find that the sublimation rate
is the same on the order of magnitude, which shows that the model is reliable in calculating the sublimation rate of
blowing snow.

Fig. 3 shows the comparison between the present and field observations at the same frictional velocity and tem-
150 perature. The red point is the snow-blowing mass concentration data on January 18, 1987 near Saskatoon (Pomero
and Male, 1992), and the black curve is the result calculated in this paper.

The suspension sublimation rate between this paper and other sublimation models under the same conditions were
also compared (Fig. 4). The black line is the sublimation rate of suspension in the case of fragmentation of snow
particles, and the other five curves are the simulation results of suspension sublimation of jump without breaking of
155 snow particles (Xiao et al., 2000; Huang and Shi, 2017). The results show that the fragmentation of snow particles
can promote the sublimation of suspension snow particles.

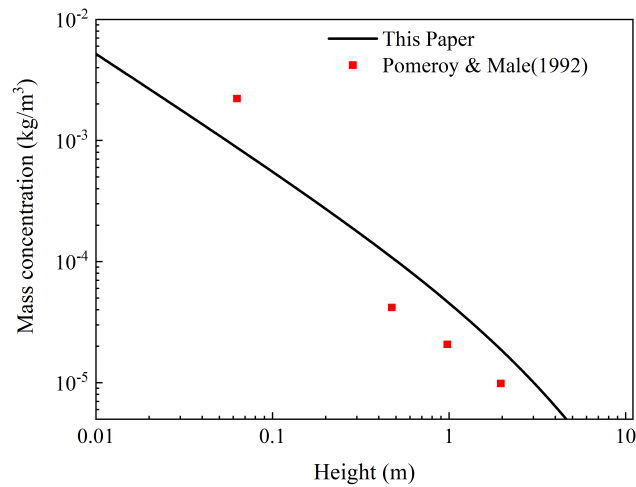


Figure 3. Comparison of mass concentration for this paper and field observation (Pomeroy and Male, 1992) ($u_* = 0.31$ m/s, $T = 265$ K)

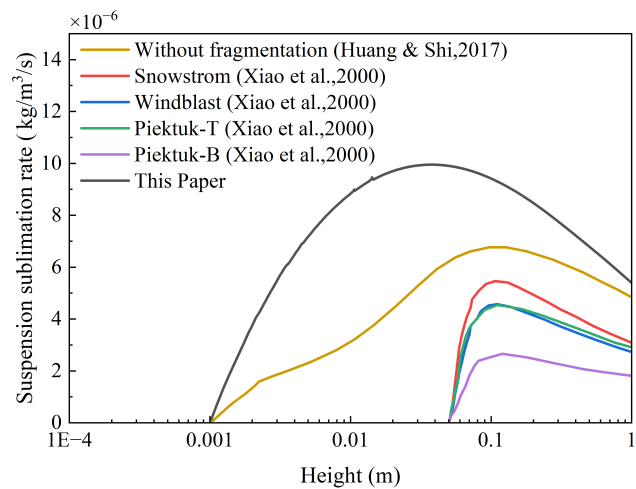


Figure 4. Comparison of the results with other five sublimation models (Xiao et al., 2000; Huang and Shi, 2017) ($u_* = 0.87$ m/s, $z_0 = 0.001$ m, $T_0 = 253.16$ K)

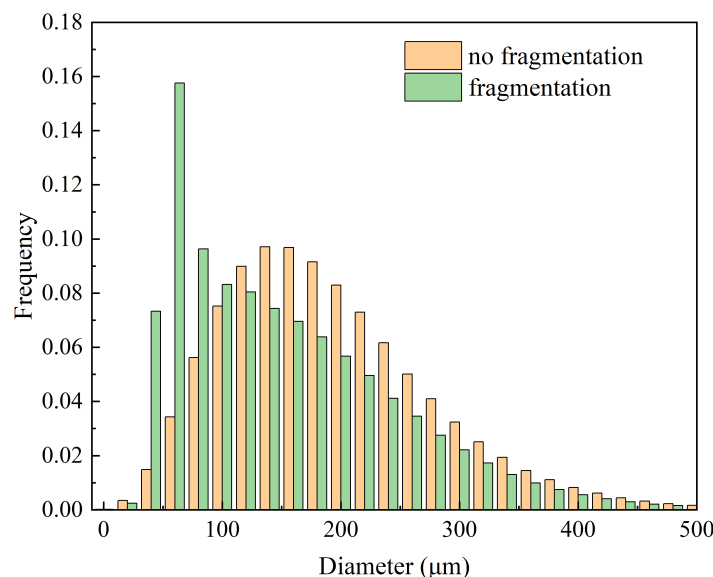


Figure 5. Size distribution with and without considering the particle fragmentation.

3 Results

3.1 Fragmentation Effects on Particle Size Distribution

The fragmentation of snow particles first leads to changes in their size distribution, releasing numerous smaller particles. Simulations were conducted to analyze the effect of fragmentation on particle size distribution.

The friction velocity $u_* = 0.45$ m/s, and the initial mean particle size $\bar{d} = 200$ μm . As shown in Fig. 5, the size distribution pattern for particles, without considering fragmentation, follows the normal distribution function (yellow bar). When considering fragmentation, the proportion of smaller-sized particles (< 100 μm) increases, while the overall proportion of larger-sized particles decreases. This results in a decrease in the average particle size.

3.2 Fragmentation Effects on Snow Particle Number

Fig. 6 presents the temporal evolution of the concentration of snow particles suspended in the air. It is observed that the number of saltation particles increases over time until reaching a steady state, regardless of the presence of fragmentation. It is noted that when fragmentation processes are taken into consideration, the steady-state concentration of snow particles is consistently higher at all wind speeds. Under low wind speed ($u_* = 0.3$ m/s), the amount of particle number increases 42 %. Under high wind speed ($u_* = 0.5$ m/s), the amount of particle number increases 26 %. This suggests that the fragmentation contributes to the total number of snow particles in the air. Furthermore, Fig. 6 also reveals that the increase of particle number resulting from fragmentation is notably more pronounced at lower wind speeds. However, the increase rate of the particle number is lower than that of the high



175 wind speed. This indicates that at higher wind speeds, the degree of fragmentation becomes more intense due to the transfer of kinematic energy to the internal energy of the particles. Therefore, during the processes of particle-bed surface and particle-particle collisions, the release rate of particles from snow particle fragmentation is higher under stronger wind conditions.

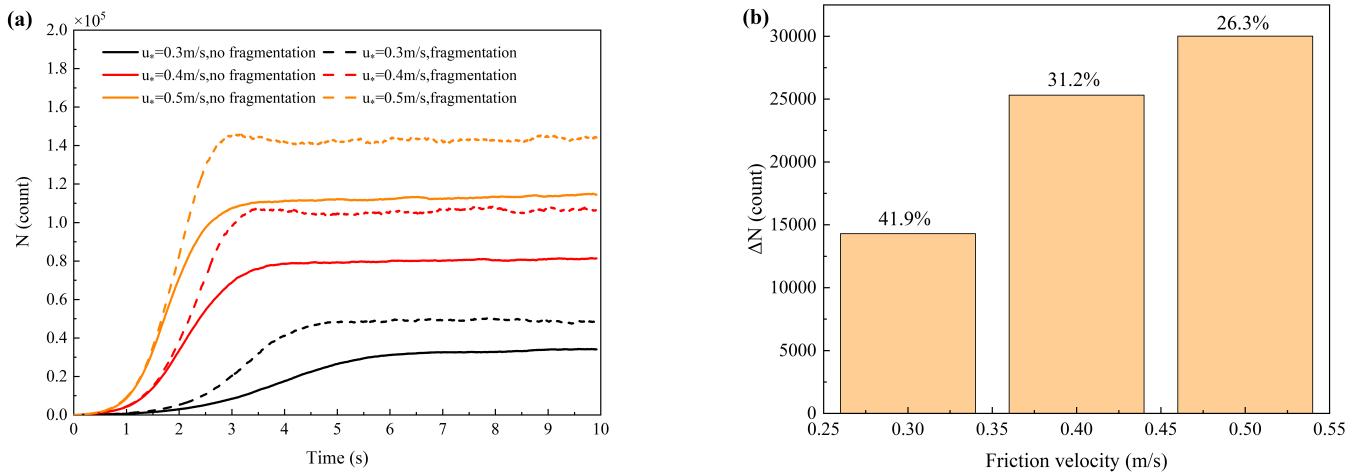


Figure 6. (a) Saltating particle number variation with time in the wind condition of $u_* = 0.3, 0.4$ and 0.5 m/s. (b) Increment number and ratios of saltation snow particles in the air.

3.3 Fragmentation Effects on Mass Concentration and Mass Flux

For near-surface saltation particles, it is illustrated in Fig. 7 that the variation in the mass concentration of saltating and suspended particles with height. The fragmentation of snow particles enhances the concentration of both saltating and suspended particles, especially at lower altitudes. Fig. 7(a) depicts the changes in mass flux along the vertical axis, showing that fragmentation enhances the transport of saltating particles near the ground surface. This is because the fragmentation of snow particles increases the number of air-borne saltation particles, more saltation particles take part in the splash process, therefore the air saltation particle number increases further. When the friction velocity varies from 0.3 m/s to 0.5 m/s, the increment proportion of fragmentation mass concentration increases from 19% to 3% , which means the fragmentation only has strong effects on the mass concentration under weak wind conditions.

For high-air suspended particles, it is shown in Fig. 7(b) that the mass concentration of the suspension snow particles in the air is higher, when considering snow particle fragmentation. This is because it is small particles that can be released from the snow fragmentation, which have more possibility to enter and being suspended in higher air.

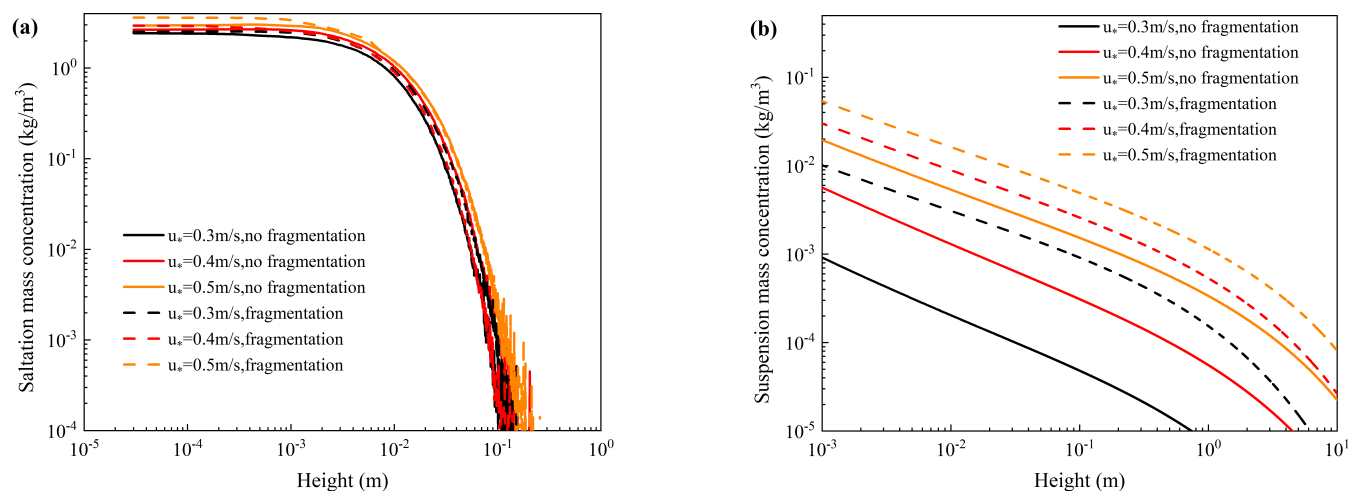


Figure 7. Mass concentration of (a) saltating and (b) suspension particles with/without considering fragmentation, in the wind condition of $u_* = 0.3, 0.4$ and 0.5 m/s.

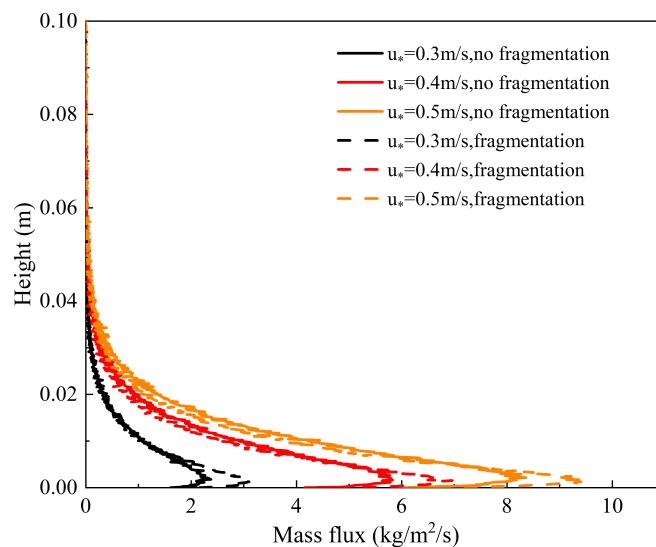


Figure 8. Mass flux distribution of snow particles with/without considering fragmentation, in the wind condition of $u_* = 0.3, 0.4$ and 0.5 m/s.

Under the same friction velocity, the mass flux of near-surface (< 0.01 m) snow particles is higher than that when considering the snow fragmentation, as is shown in Fig. 8. It can be concluded that the fragmentation increases the particles transportation of snow particles.



195 3.4 Fragmentation effects on Sublimation Rate

The sublimation rates of saltating and suspended snow particles increase with fragmentation, as shown in Fig. 9. This enhancement is more significant at lower wind speeds, indicating that snow particle fragmentation has a more profound effect on sublimation under such conditions. The sublimation rate of saltation particles increases from 16 % to 6 % when the friction velocity increases from 0.3 m/s to 0.5 m/s, considering the fragmentation effects. For 200 sublimation particles, the sublimation rate also decreases with the wind. The sublimation rate of suspension particles increases from 81 % to 70 %, considering fragmentation, which is much higher than that for saltation particles. This indicates that snow fragmentation has more fundamental effects on the sublimation process of suspension particles.

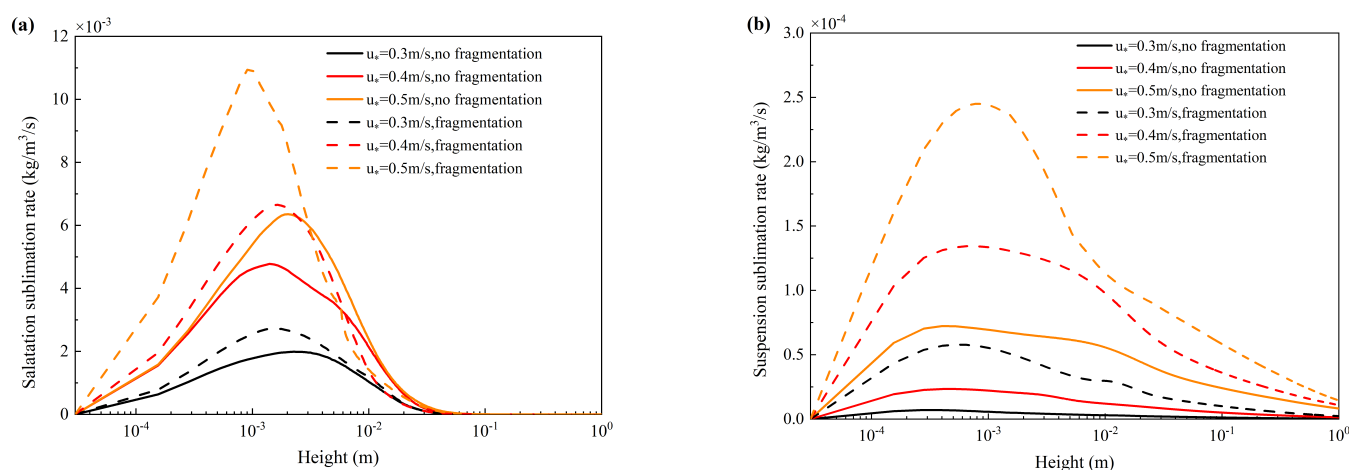


Figure 9. Sublimation rate varies with height. (a) Saltation particles. (b) Suspension particles.

3.5 Effects of Size Distribution on Fragmentation

Here, the averaged particle diameter $\bar{d} = \alpha \times \beta$. In which, α is the shape parameter. α adjusts the peak position of the curve and the steep extent of the curve. β is scale parameter, and they control width of size distribution (higher the value is, wider the size distributes).

3.5.1 Average Particle Diameter

As is shown in Fig. 10(a) or (b), with the increasing value of α or β , the number of fragmented snow particles increases, and the fragmentation efficiency is higher. This indicates that the larger particles have a higher fragment 210 extent, and this is because larger particles can produce more small snow particles.

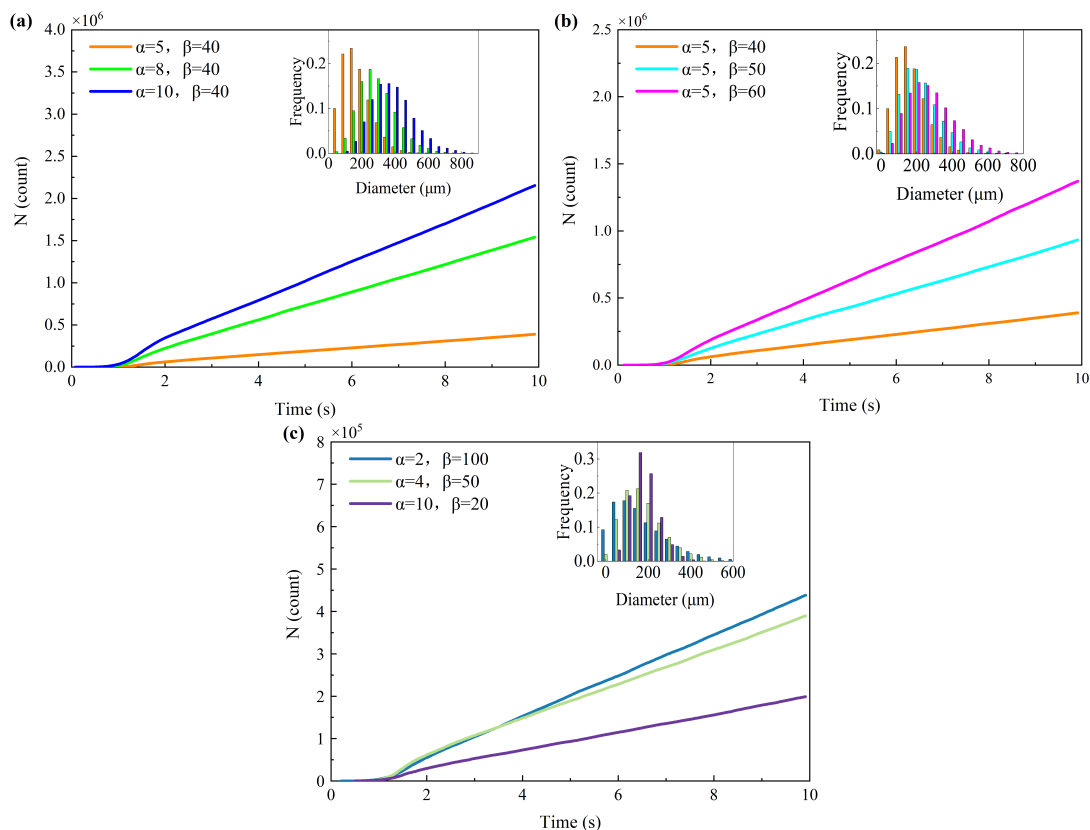


Figure 10. Number of snow particles varies with time. (a) Scale parameter $\beta = 40$. (b) Shape parameter $\alpha = 5$. (c) Average diameter $\bar{d} = 200 \mu\text{m}$

3.5.2 Size Proportion

Here we chose three different values of β with the same mean diameter $\bar{d} = 200 \mu\text{m}$. In these three cases, the the proportion of the particles larger than the threshold diameter is 73 % (blue), 85 % (green) and 96 % (purple).

As shown in Fig. 10(c), the fragmentation is significant under the same mean averaged diameter when the large
 215 particles take a higher proportion in a granular system. The fragmentation number of snow particles with different particle size distribution increases almost linearly with the time. This is because, only snow particles with a larger size than threshold diameter, more snow particles will join the fragmentation.

4 Conclusion

This work investigated the significant role of snow particle fragmentation on drifting snow and blowing snow. We
 220 found that fragmentation not only alters the particle size distribution, but also increases the number, concentration



and mass flux of snow particles. Subsequently, this phenomenon affects the sublimation rate of air-moving snow particles.

Our results show that fragmentation diminishes the particle size on average, which provides more opportunities for smaller particles to sublimate. With consideration of particle fragmentation, the amount of particle mass concentration and sublimation rate increases one order of magnitude when considering particle fragmentation, which indicates fragmentation of saltation snow particles is one of the fundamental sources of suspended snow particles. The sublimation rate of saltating snow particles increases 11 % on average, and that of suspension snow particles increases 76 % on average when the friction wind speed is between 0.3 m/s to 0.5 m/s. The differences in sublimation rate with/without considering fragmentation decrease with increasing wind speeds. We also investigated the effects of size distribution of particles on the sublimation rates. We found that the sublimation rate is enhanced when the particles with a larger average diameter and a higher proportion of larger particles.

Our simulation results are consistent with the previous observation results, which indicates the validity of our model. Furthermore, compared with the calculating results from the model which does not consider fragmentation of snow particles, our sublimation rates are 2-4 times higher than the previous model results. This is because fragmentation diminishes the snow particle's size, and smaller snow particles are more prone to sublimate in the air.

Our work provides insights into the complex dynamics of drifting and blowing snow. It provides a deeper understanding of the physical process of snow particle fragmentation during saltating/suspending in the air. This indicates the importance of fragmentation in the drifting and blowing snow numerical model. However, this model is a two-dimensional numerical model, which could not be applied to larger regions, especially for complex terrains. Therefore, the implementation of this model into a three-dimensional drifting snow model in the future is necessary.

The results provide detailed physical dynamic processes of particle-atmospheric momentum transfer, heat transfer, and mass transfer, from each single particle aspect. This supplies the theoretical basement and prediction methods for assessing the accurate amount of snow sublimation during drifting and blowing snow, which should be further implemented in more related atmospheric and climate models.

Author contributions. HX Y contributed to the conception and first draft, JC B contributed to the programing and numerical calculation, N H and G L designed the conception and revised the manuscript.

Competing interests. All authors declare that no competing interests are present.

Acknowledgements. This work was supported by the Third Comprehensive Scientific Expedition and Research Program in Xinjiang (grant no.: 2022xjkk0101), the National Natural Science Foundation of China (grant no.: 42476251, 42406255), the



- 250 China Postdoctoral Science Foundation (grant no.: 2024M751257). The data and code will be uploaded to the Dryad repository after the paper is published.



References

- Anderson, R. S. and Haff, P. K.: Wind modification and bed response during saltation of sand in air, *Acta Mechanica Suppl.*, 1, 21–51, 1991.
- 255 Bintanja, R.: Snowdrift suspension and atmospheric turbulence. Part I: Theoretical background and model description., 2000b.
- Comola, F., Kok, J., Gaume, J., Paterna, E., and Lehning, M.: Fragmentation of wind-blown snow crystals: Blowing snow fragmentation, *Geophysical Research Letters*, 44, <https://doi.org/10.1002/2017GL073039>, 2017.
- Csanady, G. T.: Turbulent Diffusion of Heavy Particles in the Atmosphere, *Journal of Atmospheric Sciences*, 20, 201 – 208, [https://doi.org/10.1175/1520-0469\(1963\)020<0201:TDOHPI>2.0.CO;2](https://doi.org/10.1175/1520-0469(1963)020<0201:TDOHPI>2.0.CO;2), 1963.
- 260 Dai, X. and Huang, N.: Numerical simulation of drifting snow sublimation in the saltation layer, *Scientific Reports*, 4, <https://api.semanticscholar.org/CorpusID:14720403>, 2014.
- Domine, F., Salvatori, R., Legagneux, L., Salzano, R., Fily, M., and Casacchia, R.: Correlation between the specific surface area and the short wave infrared (SWIR) reflectance of snow, *Cold Regions Science and Technology*, 46, 60–68, <https://doi.org/https://doi.org/10.1016/j.coldregions.2006.06.002>, 2006.
- 265 Domine, F., Taillandier, A.-S., Cabanes, A., Douglas, T. A., and Sturm, M.: Three examples where the specific surface area of snow increased over time, *The Cryosphere*, 3, 31–39, <https://doi.org/10.5194/tc-3-31-2009>, 2009.
- Déry, S. J. and Yau, M. K.: Large-scale mass balance effects of blowing snow and surface sublimation, *Journal of Geophysical Research: Atmospheres*, 107, ACL 8–1–ACL 8–17, <https://doi.org/https://doi.org/10.1029/2001JD001251>, 2002.
- Huang, N. and Shi, G.: The significance of vertical moisture diffusion on drifting Snow sublimation near snow surface, *The*
- 270 *Cryosphere Discussions*, pp. 1–28, <https://doi.org/10.5194/tc-2017-116>, 2017.
- Nemoto, M. and Nishimura, K.: Numerical simulation of snow saltation and suspension in a turbulent boundary layer, *Journal of Geophysical Research: Atmospheres*, 109, <https://doi.org/https://doi.org/10.1029/2004JD004657>, 2004.
- Pomeroy, J. and Male, D.: Steady-state suspension of snow, *Journal of Hydrology*, 136, 275–301, [https://doi.org/https://doi.org/10.1016/0022-1694\(92\)90015-N](https://doi.org/https://doi.org/10.1016/0022-1694(92)90015-N), 1992.
- 275 Pomeroy, J. W. and Jones, H. G.: Wind-Blown Snow: Sublimation, Transport and Changes to Polar Snow, <https://api.semanticscholar.org/CorpusID:11700473>, 1996.
- Sato, T., Kosugi, K., Mochizuki, S., and Nemoto, M.: Wind speed dependences of fracture and accumulation of snowflakes on snow surface, *Cold Regions Science and Technology*, 51, 229–239, <https://doi.org/https://doi.org/10.1016/j.coldregions.2007.05.004>, international Snow Science Workshop (ISSW) 2006,
- 280 2008.
- Schmidt, R. A.: Vertical profiles of wind speed, snow concentration, and humidity in blowing snow, *Boundary-Layer Meteorology*, 23, 223–246, 1982.
- Scott, W. D.: Measuring the erosivity of the wind, *CATENA*, 24, 163–175, [https://doi.org/https://doi.org/10.1016/0341-8162\(95\)00022-K](https://doi.org/https://doi.org/10.1016/0341-8162(95)00022-K), 1995.
- 285 Sugiura, K. and Maeno, N.: Wind-Tunnel Measurements Of Restitution Coefficients And Ejection Number Of Snow Particles In Drifting Snow: Determination Of Splash Functions, *Boundary-Layer Meteorology*, 95, 123–143, <https://doi.org/10.1023/A:1002681026929>, 2000.



- Thorpe, A. D. and Mason, B. J.: The evaporation of ice spheres and ice crystals, *British Journal of Applied Physics*, 17, 541, <https://doi.org/10.1088/0508-3443/17/4/316>, 1966.
- 290 Ueno, K., Tanaka, K., Tsutsui, H., and Li, M.: Snow cover conditions in the Tibetan Plateau observed during the winter of 2003/2004, *ARCTIC ANTARCTIC AND ALPINE RESEARCH*, 39, 152–164, [https://doi.org/10.1657/1523-0430\(2007\)39\[152:SCCITT\]2.0.CO;2](https://doi.org/10.1657/1523-0430(2007)39[152:SCCITT]2.0.CO;2), 2007.
- Walter, B., Weigel, H., Wahl, S., and Löwe, H.: Wind tunnel experiments to quantify the effect of aeolian snow transport on the surface snow microstructure, *The Cryosphere*, 18, 3633–3652, <https://doi.org/10.5194/tc-18-3633-2024>, 2024.
- 295 Xiao, J., Bintanja, R., Déry, S., Mann, G., and Taylor, P.: An Intercomparison Among Four Models Of Blowing Snow, *Boundary-Layer Meteorology*, 97, 109–135, <https://doi.org/10.1023/A:1002795531073>, 2000.